Lestinen, Sami; Kilpeläinen, Simo; Kosonen, Risto; Jokisalo, Juha; Koskela, Hannu

An experimental study on airflow characteristics and thermal environment with asymmetrically located heat loads and low-momentum diffuse ceiling ventilation.

Published in:
Proceedings of Roomvent & Ventilation 2018, 2-5th of June 2018, Espoo, Finland

Published: 05/06/2018

Document Version
Publisher's PDF, also known as Version of record

Please cite the original version:
Lestinen, S., Kilpeläinen, S., Kosonen, R., Jokisalo, J., & Koskela, H. (2018). An experimental study on airflow characteristics and thermal environment with asymmetrically located heat loads and low-momentum diffuse ceiling ventilation. In *Proceedings of Roomvent & Ventilation 2018, 2-5th of June 2018, Espoo, Finland* SIY Sisäilmatieto Oy.

AN EXPERIMENTAL STUDY ON AIRFLOW CHARACTERISTICS AND THERMAL ENVIRONMENT WITH ASYMMETRICALLY LOCATED HEAT LOADS AND LOW-MOMENTUM DIFFUSE CEILING VENTILATION

Sami Lestinen[1,*], Simo Kilpeläinen[1], Risto Kosonen[1], Juha Jokisalo[1], Hannu Koskela[2]
[1]Aalto University, Espoo, Finland
[2]Turku University of Applied Sciences, Turku, Finland
[*]*Corresponding email: sami.lestinen@aalto.fi*

SUMMARY

Airflow characteristics were studied with asymmetrical heat load distribution and diffuse ceiling ventilation. The heat load was increased from 40 W/floor-m^2 to 80 W/floor-m^2, while the average air temperature was kept at 26±0.5°C. Experiments were carried out in a test chamber of 5.5 m length x 3.8 m width x 3.2 m height with omnidirectional anemometers by 1-hour interval. The heat loads consisted of two opposite workstations next to warm window panels in the perimeter area. The other side of the room was an open area describing a corridor zone. Both workstations had a seated test dummy with a laptop and a monitor. The results indicate that the mean air speed and the airflow fluctuation increase with heat load. Consequently, also the turbulent kinetic energy and the turbulence dissipation increase. However, the increased heat load had only a small effect on turbulence intensity. Therefore, draught rate increased significantly with mean air speed. In addition, the smallest length-scale decreased towards increased heat load. This thermal environment would be classified as the category B-C defined by the European Standard EN ISO 7730:2005, because the mean air speed levels were too high at increased heat load conditions.

Keywords: thermal environment, heat load, buoyancy flows, airflow interaction, diffuse ceiling ventilation

1 INTRODUCTION

Understanding building characteristics may provide healthier and more comfortable buildings (Sakellaris et al., 2016). This includes also thermal conditions and draught. Draught is defined as an unwanted local cooling of a person (Fanger, 1970). An airflow with high turbulence causes more complaints of draught than an airflow with low turbulence at the same mean velocity and air temperature (Fanger et al., 1988). The risk of draught increases when the airflow temperature decreases and the mean velocity and the turbulence intensity increase (Müller et al., 2013). Consequently, advanced air distribution methods can improve thermal comfort and energy efficiency (Melikov, 2016). In addition, thermal conditions has been shown to affect the performance and learning (Wargocki and Wyon, 2017).

Scientific evidence shows that ventilation is essential for good indoor environmental quality (Seppänen, 2008). Consequently, air distribution is one of the major factors for health, comfort and performance (Müller et al., 2013). In addition, draught has been a common complaint in the buildings (Kosonen et al., 2011; Sakellaris et al., 2016). Generally, the room airflow pattern depends on the relative locations of air distribution units and heat sources (Koskela et al., 2010). Furthermore, indoor airflows are difficult to predict in advance. Therefore, the draught can be a common complaint also in the modern offices.

In this study, the objective is to investigate the effects of increased heat load on airflow characteristics with diffuse ceiling ventilation, in which an even supply of perforated suspended ceiling penetrates supply air down to the occupied zone instead of local supply openings (Zhang et al., 2014). The diffuse ceiling inlet can handle high heat loads without a significant draught, hence disturbing only a little the buoyancy flows from the heat sources (Nielsen, 2017). Novelty of the study comes from systematic investigation and detailed analysis of time and spatial averaged dataset records to discover effects on seated person zone with asymmetrical heat load setup.

2 METHODS

Internal dimensions of the test chamber were 5.5 m length, 3.8 m width and 3.2 m height. The test case parameters are shown in Table 1.

Table 1. Test case parameters. Floor area 21 m^2.

Test cases	C40	C80
Heat load [W/floor-m^2]	40±2	80±4
Average air temperature [°C]	26±0.5	26±0.5
Supply airflow rate [l/s,m^2]	3.6±0.2	7.3±0.4
Supply air temperature [°C]	17±0.1	17±0.1

The experimental set-up consisted of double office layout (Figure 1ab). The workstation consisted of a seated test dummy (90±5 W) with a laptop (48±3 W) and a monitor (35±2 W). A table was located 0.6 m from the heated window panels at width-coordinate of 3.8 m (Figure 1ab). Lights (116±6 W) were installed in the middle of the workstations at height 3.2 m. Heating foil (420±21 W, 5x1 m^2, LxW) was installed on the floor 0.8 m from the windows. A heat source of 0.4x0.4x0.4 m^3 (103±5 W) was located under the table for a peak load (Figure 1a, rectangle near loc. 13). A window panel dimensions were 0.6x1.8 m^2, WxH. The window surface temperature was set at 30-40°C such that a target heat load was achieved.

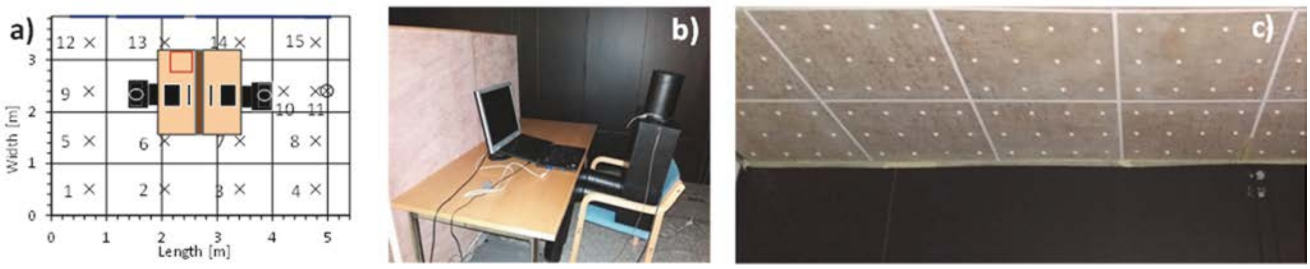

Figure 1. Test chamber: a) the measurement locations 1-15, b) the workstation and c) the diffuse ceiling inlet with the perforation rate of 0.50±0.02 %.

Supply air was discharged through the diffused ceiling down to the occupied zone. The perforation rate was 0.50±0.02 % with a nozzle diameter of 14 mm (Figure 1c). The nozzle row closest to each wall was sealed. The air was extracted from the height of 3.2 m (Figure 1a, circle at loc. 11). The anemometers (Table 2) were installed at heights 0.1 m, 0.6 m, 1.1 m, 1.4 m, 1.7 m, 2.3 m and 2.9 m recommended by EN ISO 7726:2001 (CEN, 2001). The sampling rate was 10 Hz in the seated person zone below the height of 1.1 m and 0.5 Hz in the upper zone. The averaging interval was 1 hour.

Table 2. Measuring equipment.

Variable	Meter	Model	Accuracy
Air temperature Air speed (at height 0.1 m-1.1 m)	Omnidirectional anemometer	Dantec dynamics Vivo Draught 20T31	Air speed (v) ±0.01 m/s±0.025v Air temperature ±0.15°C STDerr < 10 % to 2 Hz
Air temperature Air speed (at height 1.4 m-2.9 m)	Omnidirectional anemometer	Sensor electronic SensoAnemo 5100SF	Air speed (v) ±0.02 m/s±0.015v Air temperature ±0.2°C STDerr < 10 % to 1.5 Hz

The draught rate defined by EN ISO 7730:2005 is expressed as

$$DR = \left(34 - t_{a,l}\right)\left(\bar{U}_{a,l} - 0.05\right)^{0.62}\left(0.37 \cdot \bar{U}_{a,l} \cdot Tu + 3.14\right) \tag{1}$$

where $t_{a,l}$ [°C] is the local air temperature, $\bar{U}_{a,l}$ [m/s] is the local mean air velocity, and Tu [%] is the local turbulence intensity. The turbulence intensity Tu, turbulent kinetic energy k_t, turbulence dissipation ε and the Kolmogorov length scale l_η are written as

$$Tu = \frac{U_{\mathrm{std}}}{\bar{U}} \times 100; \quad k_t = \frac{1}{2}\overline{U'U'}; \quad \varepsilon = \frac{{k_t}^{3/2}}{l}; \quad l_\eta = \left(\frac{\nu^3}{\varepsilon}\right)^{1/4} \tag{2}$$

where U_{std} is the standard deviation of instantaneous air speed, $\bar{U}$ is the mean air speed. U' is the fluctuating component of air speed, l is the largest length scale (here l=3 m) and ν is the kinematic viscosity.

3 RESULTS

The room average air temperature was 25.6°C at 40 W/floor-m^2 (C40) and 26.0°C at 80 W/floor-m^2 (C80) (Figure 2a). The mean air temperatures ranged from 25.1°C to 26.9°C at C40 and from 24.6°C to 27.1°C at C80, thus the range was 1.8°C and 2.5°C, respectively (Figure 2b). In the seated person zone (below 1.1 m), the corresponding ranges were lower 1.7°C and 2.0°C, respectively. The air temperature was higher in the window side than in the corridor side (Figure 2c) and the average vertical difference was small. However, local differences existed. The maximum difference between the heights was 1.1°C at C40 at location 13 (Figure 1) and 0.8°C at C80 at location 8 in the seated person zone.

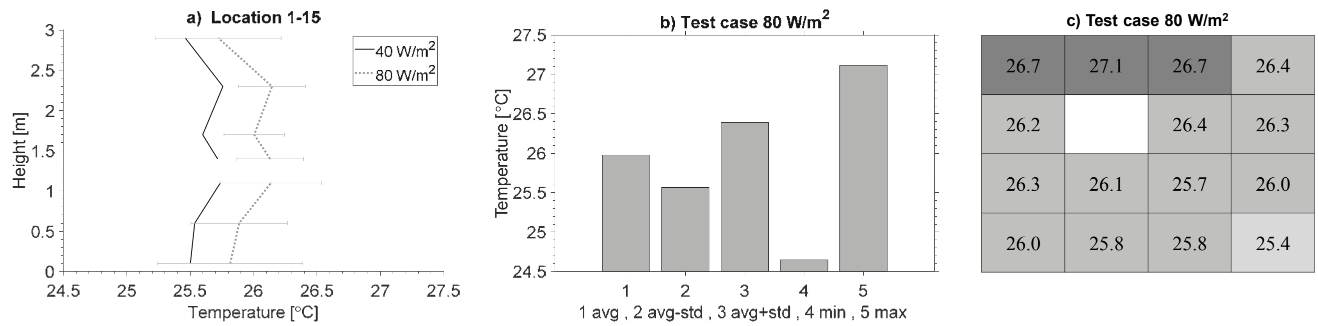

Figure 2. The air temperature: a) The average air temperature at C40 and C80, error bars indicate ±std. b) The air temperature statistics at C80. c) The maximum air temperature in the seated person zone below 1.1 m at the locations 1-15 (Figure 1a). The light grey at T≤25.5°C, the medium grey at 25.5<T<26.5°C and the dark grey at T≥26.5°C.

The mean air speed and the deviation of mean air speed increased with heat load (Figure 3a). In the seated person zone, the average air speed was 0.12±0.05 m/s (±std) at C40 and 0.16±0.07 m/s at C80. The highest air speed was observed near the floor and lowest at the head level in the seated person zone. The vertical mean air speed gradient was greater in the middle of the test chamber than in the window side or in the corridor side (Figure 3b). In addition, the maximum air speed level was higher in the corridor side than in the window side regarding the seated person zone (Figure 3c).

The heat load had only a small effect on the turbulence intensity (Figure 4a). However, the lowest average intensity was obtained near the floor and the highest intensity was found near the head level in the seated person zone at the height or 1.1 m. Furthermore, the average turbulence intensity was higher in the middle of the test chamber (loc. 5-8) than in the window side (loc. 12-15) or in the corridor side (loc. 1-4) (Figure 4b). The local maximums ranged from 40 % to 84 % at C80 in the seated person zone (Figure 4c).

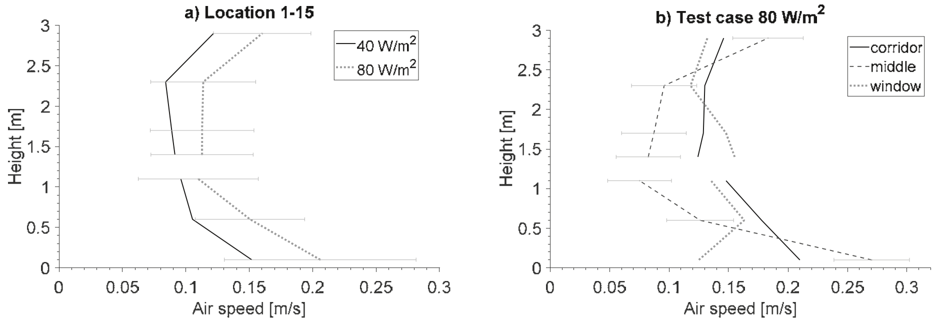

c) Test case 80 W/m²

0.16	0.21	0.14	0.15
0.27		0.16	0.30
0.22	0.32	0.24	0.31
0.26	0.23	0.19	0.20

Figure 3. a) The average air speed at C40 and C80, error bar denotes ±std. b) The average air speed in the corridor side (loc. 1-4), middle (loc. 5-8) and window side (loc. 12-15), error bar denotes uncertainty in measurement. c) Maximum mean air speed of the locations 1-15 (Figure 1a) below 1.1 m. The light grey at $\overline{U}$<0.2 m/s, the medium grey at 0.2≤$\overline{U}$<0.3 m/s and the dark grey at $\overline{U}$≥0.3 m/s.

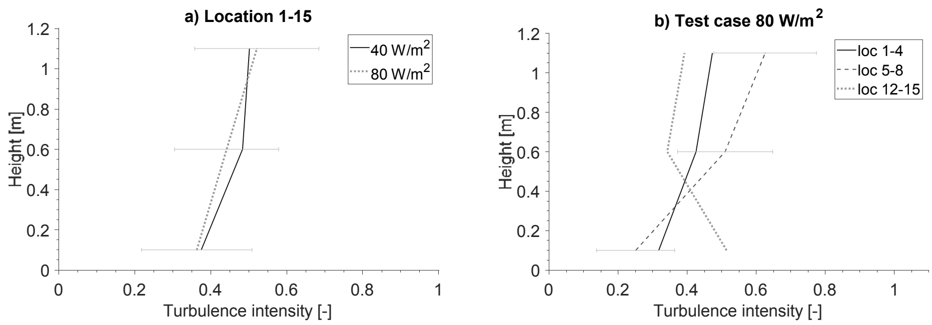

c) Test case 80 W/m²

49	49	54	54
73		65	64
84	45	43	81
63	45	59	40

Figure 4. a) The turbulence intensity at C40 and C80, error bars ±std. b) The average turbulence intensity in the corridor side (loc. 1-4), middle (loc. 5-8) and window side (loc. 12-15), error bar denotes uncertainty in measurement. c) The maximum turbulence intensity below 1.1 m. The light grey at Tu≤40 %, the medium grey at 40<Tu<60 % and the dark grey at Tu≥60 %.

The average draught rate was largest near the floor and smallest at the head level in the seated person zone (Figure 5a). The draught rate and the deviation increased with heat load (Figure 5b). Furthermore, the local maximum ranged 9-21 % at C80 in the seated person zone (Figure 5c). The average draught rate was higher in the corridor side than in the window side near the heat sources.

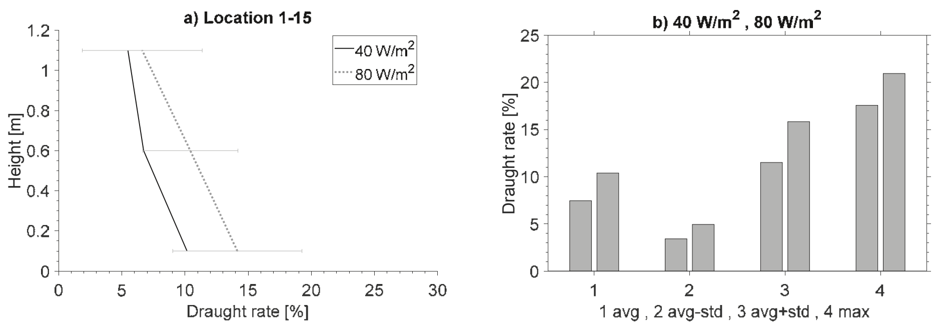

c) Test case 80 W/m²

10	12	9	10
18		12	19
16	21	17	20
18	17	14	16

Figure 5. a) The draught rate at C40 and C80 in the seated person zone, error bars ±std. b) The statistics of draught rate below 1.1 m. c) The maximum draught rate below 1.1 m. The light grey is category A (DR<10 %), medium grey is category B (DR<20 %) and dark grey is category C (DR<30 %) defined by EN ISO 7730:2005 (CEN, 2005).

The average turbulent kinetic energy increased with heat load (Figure 6a). The highest turbulent kinetic energy level was observed near the floor in which the average air speed level was highest. Consequently, also the turbulence dissipation increased correspondingly (Figure 6b). The turbulence length scales ranged from the room size down to the millimetres. The largest length scale was around the room height based on marker smoke visualization. The smallest length scale decreased towards increased heat load (Figure 6c).

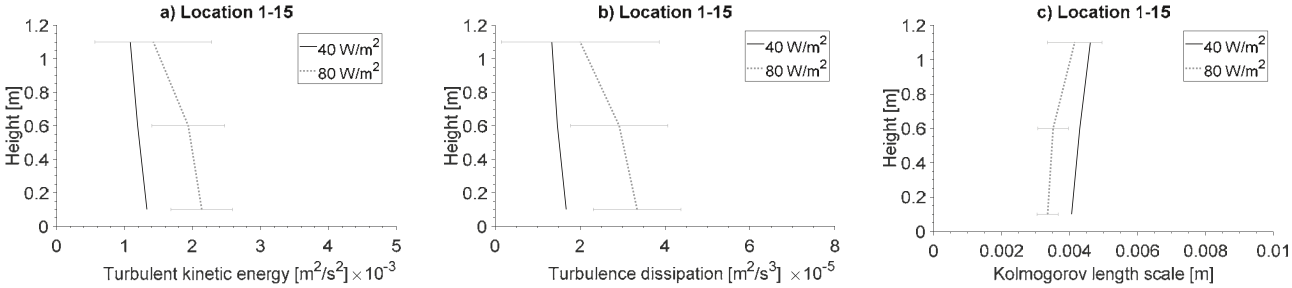

Figure 6. a) The turbulent kinetic energy at C40 and C80. b) The turbulence dissipation at C40 and C80. c) The Kolmogorov length scale at C40 and C80. The error bars denote ±std.

4 DISCUSSION

The ranges of mean air temperatures were 1.7°C and 2.0°C in the seated person zone at C40 and C80, respectively. This indicates significant air temperature differences with peak load conditions. The maximum vertical difference of air temperatures was observed above and below the table at the location 13 at C40 such that the lower air temperature was below the table. Most probably, this is due to relative locations of heat sources and tables, which block the airflow patterns. Therefore, further question is settled to consider a detailed flow field of workstation in the future. The mean air speed and the deviation of mean air speed increased with heat load. The greatest averaged air speed gradients were observed in the middle of the chamber (loc. 5-8). Most probably, this is due to the large-scale circulating airflow pattern from the window side to the opposite corridor side that was obtained with marker smoke. The head load had a small effect on turbulence intensity, probably because both the standard deviation of air speed and the mean air speed increased with heat load. Furthermore, the lowest intensity was obtained in the high air speed conditions and the corresponding highest intensity in the low air speed conditions, because the deviation of air speed may decrease less than the mean air speed under the low air speed conditions. The heat load increased the turbulent kinetic energy and dissipation. The highest turbulent kinetic energy level was observed near the floor where the mean air speed level was highest, because the velocity fluctuation increased with mean air speed. Therefore, also the average turbulence dissipation increased. The largest length scale was around room height based on marker smoke visualization. The smallest length scale decreased towards increased heat load, because the turbulence dissipation increased with heat load. The draught rate increased with heat load indicating the category B at C40 and the category C at C80 defined by EN ISO 7730:2005 (CEN, 2005). However, an uncertainty in measurement can be around 5 % p.p. (Melikov et al., 2007), thus uncertainty in category exists correspondingly. The category A was not achieved, because the air speed was too high with the given heat loads. Consequently, the design criteria is proposed to be further considered for the indoor environments with increased heat loads, e.g. for the kindergartens in the standard EN ISO 7730:2005.

5 CONCLUSIONS

The temperature variation was significant in the seated person zone, although the average air temperature reached the target level. The mean air speed and the deviation of mean air speed increased with heat load. However, the heat load had a small effect on turbulence intensity. The local maximum of draught rate indicates that this thermal environment has category B at C40 and category C at C80 defined by EN ISO 7730:2005. The category A was not achieved, because the air speed was too high with the given heat loads. Both the turbulent kinetic energy and dissipation increased with heat load. In addition, the smallest turbulence length scale decreased when the heat load increased.

ACKNOWLEDGEMENTS

The authors wish to acknowledge Foundation LVY for financial support, Professor Dr. Arsen Melikov from the Technical University of Denmark and Professor Dr. Mats Sandberg from the University of Gävle, Sweden for discussion and comments. The authors would also like to express gratitude to Mr. Etienne Daviet from the Institute National des Sciences Appliquées in Lyon, France, for contributing to the measurements.

REFERENCES

CEN (2001). European Standard EN ISO 7726:2001, Ergonomics of the thermal environment. Instruments for measuring physical quantities.

CEN (2005). European Standard EN ISO 7730:2005, Ergonomics of the thermal environment — Analytical determination and interpretation of thermal comfort using calculation of the PMV and PPD indices and local thermal comfort criteria.

Fanger, P O. (1970). Thermal Comfort. Danish Technical Press.

Fanger, P.O., A.K. Melikov, H. Hanzawa, and J. Ring. 1988. Air turbulence and sensation of draught. Energy and buildings, 12(1), 21-39.

Koskela, H., Häggblom, H., Kosonen, R., and Ruponen, M. (2010). Air distribution in office environment with asymmetric workstation layout using chilled beams. Building and Environment, 45(9), 1923-1931.

Kosonen, R., Ahola, M., Villberg, K., and Takki, T. (2011). Perceived IEQ conditions: why the actual percentage of dissatisfied persons is higher than standards indicate? Sick Building Syndrome, Springer Berlin Heidelberg, 2011, pp. 75–88.

Melikov, A. K. (2016). Advanced air distribution: Improving health and comfort while reducing energy use. Indoor air, 26(1), 112-124.

Melikov, A. K., Popiolek, Z., Silva, M. C. G., Care, I., and Sefker, T. (2007). Accuracy limitations for low-velocity measurements and draft assessment in rooms. HVAC&R Research, 13(6), 971-986.

Müller, D., Kandzia, C., Kosonen, R., Melikov, A. K., and Nielsen, P. V. (2013). Mixing Ventilation. Guide on mixing air distribution design. Federation of European Heating and Air-Conditioning Associations, REHVA.

Nielsen, P. V., Vilsbøll, R. W., Liu, L., & Jensen, R. L. (2017). Diffuse Ceiling Ventilation, Load Distribution and Ceiling Design. Proceedings of Healthy Buildings Europe, Lublin, Poland.

Sakellaris, I. A., D.E. Saraga, C. Mandin, C. Roda, S. Fossati, Y. de Kluizenaar, ... and O. Hänninen. 2016. Perceived indoor environment and occupants' comfort in European "modern" office buildings: the OFFICAIR study. International journal of environmental research and public health, 13(5), 444.

Seppänen, O. (2008). Scientific basis for design of ventilation for health, productivity and good energy efficiency. In Proceedings of the international conference on indoor air quality and climate, Copenhagen, Denmark.

Wargocki, P., and Wyon, D. P. (2017). Ten questions concerning thermal and indoor air quality effects on the performance of office work and schoolwork. Building and Environment, 112, 359-366.

Zhang, C., Heiselberg, P., and Nielsen, P. V. (2014). Diffuse Ceiling Ventilation-A Review. International Journal of Ventilation, 13(1), 49-63.